

First-order phase transition in a gauge theory of $S = 1/2$ quantum antiferromagnets in the deep easy-plane limit

S. Kragset,¹ E. Smørgrav,¹ J. Hove,¹ F. S. Nogueira,² and A. Sudbø^{1,3}

¹ Department of Physics, Norwegian University of Science and Technology, N-7491 Trondheim, Norway

²Institut für Theoretische Physik, Freie Universität Berlin, Arnimallee 14, D-14195 Berlin, Germany

³Centre for Advanced Study at the Norwegian Academy of Science and Letters, Drammensveien 78, N-0271 Oslo, Norway

We perform large-scale Monte Carlo simulations on an effective gauge theory for a deep easy-plane antiferromagnet, including a Berry phase term that projects out the $S = 1/2$ sector. Without a Berry phase term, the model exhibits a phase transition in the $3DXY$ universality class associated with proliferation of gauge-charge neutral $U(1)$ vortices. The instantons that eliminate the phase transition in the gauge-charged sector are suppressed by the Berry phases. The result is a *first-order* phase transition.

PACS numbers: 73.43.Nq, 75.10.Jm, 11.15.Ha

The Landau–Ginzburg–Wilson (LGW) theory for phase transitions has been an immensely successful paradigm of physics for the last 50 years. It is one of the cornerstones of statistical and condensed matter physics, providing deep insight into phase transitions [1]. The standard example is the well-known paramagnetic–ferromagnetic phase transition. Recently, examples of phase transitions that do not fit into the LGW paradigm have been discussed [2, 3, 4]. These are specific *continuous* quantum phase transitions from a Néel state with conventional antiferromagnetic order into a paramagnetic valence-bond solid (VBS) state [5]. In the Néel state, an $SU(2)$ symmetry is broken, while in the valence-bond solid translational symmetry is broken. Hence, the phase transition separating them is an order–order phase transition with two distinct order parameters associated with it. Continuous order–order phase transitions would not easily fall within the LGW paradigm, where this type of transitions are typically first-order.

An attempt to provide proof of evidence for these ideas has recently been put forth [2]. It involves a deformation of the Heisenberg model into an easy-plane quantum antiferromagnet. The latter can be studied through the deep easy-plane version of an effective lattice gauge theory for a quantum antiferromagnet proposed in Ref. [6]. For $S = 1/2$ it has the action

$$S[\theta, \mathbf{A}; \eta] = \sum_j \left[\sum_{\mu=1}^3 \left(\beta \sum_{a=1}^2 [1 - \cos(\Delta_\mu \theta_{ja} - A_{j\mu})] + \kappa \{1 - \cos[(\Delta \times \mathbf{A}_j)_\mu]\} \right) + i\eta_j A_{j\tau} \right]. \quad (1)$$

The first term is reminiscent of the CP^1 representation of the non-linear σ model description of a quantum antiferromagnet. There the orientation of the Néel order parameter is represented by $\mathbf{n}_j = z_{ja}^* \sigma_{ab} z_{jb}$. The deep easy-plane limit together with the constraint $|z_1|^2 + |z_2|^2 = 1$ allows us to write $z_{ja} = e^{i\theta_{ja}} / \sqrt{2}$. \mathbf{A} is a compact gauge

field which here is doing more than just being an auxiliary field, like in the case of the CP^1 model. It determines also the Berry phase for the above model. The index τ corresponds to $\mu = 3$, and the staggering factor is given by $\eta_j = \pm 1$ and is independent of imaginary time. Note that the present gauge field is a function of the space-time coordinates, in contrast to the usual Berry gauge potential appearing in $SU(2)$ spin models [4], which is a functional of the spin field.

Compactness of the gauge field gives rise to instanton configurations [7] which are known to remove a second order phase transition in a corresponding model with only one complex scalar matter field and no Berry phase [8]. Without the Berry phase and with two matter fields present, it is known that one can rewrite the theory in terms of a linear combination of phase fields which does not couple to the gauge field, and one which does [9, 10]. Thus, regardless of whether the gauge field is compact or not, the charge-neutral linear combination of phase fields features topological objects which proliferate in a $3DXY$ phase transition [10]. The remaining charged sector will behave as for the one-component case [10, 11].

Recently, it has been argued that the Berry phase, which is crucial to describe the phase inside the paramagnetic phase [2, 3], suppresses the instantons at the critical point. In a phase transition from a Néel to a VBS state, the spinons are confined at either of these phases. Irrelevance of instantons at the critical point leads to the so called “deconfined quantum criticality” [2]. Here we will investigate this point by monitoring the phase transitions in the model (1) in the presence and absence of a Berry phase term. As already mentioned, without such a term we expect a phase transition in the $3DXY$ universality class. The latter is driven by a vortex-loop proliferation in the neutral sector. In the presence of a Berry phase term, a phase transition is also expected in the charged sector. Since the bare phase stiffnesses of the two matter fields are the same, the proliferation temperature of the neutral and charged cases will also be the

same. The result will be shown to be a single first-order phase transition.

The deconfined quantum criticality scenario implies that the critical point is governed by an easy-plane system action featuring a non-compact gauge field, i.e.,

$$S[\theta, \mathbf{A}] = \sum_i \sum_{\mu=1}^3 \left\{ \beta \sum_{a=1}^2 [1 - \cos(\Delta_\mu \theta_{ia} - A_{i\mu})] + \frac{\kappa}{2} (\Delta \times \mathbf{A}_i)_\mu^2 \right\}. \quad (2)$$

This model with unequal bare phase stiffnesses has been studied in great detail [10]. It features two distinct second-order phase transitions, one belonging to the 3DXY universality class and another one corresponding to the so-called inverted 3DXY transition [12]. In the limit where the bare phase stiffnesses are equal, clear signals of non-3DXY behavior are seen [10, 13]. In Ref. 13, strong indications of a first-order phase transition in a loop-gas representation of the non-compact model Eq. (2), were found. We will consider both Eqs. (1) and (2) in detailed Monte Carlo (MC) simulations.

For performing MC simulations on the model with a Berry phase term, it is convenient to introduce a dual representation of the model Eq. (1). In such a representation the action is real, given by [4]

$$S[\mathbf{h}^{(a)}, s; f] = \frac{1}{2} \sum_i \left\{ \frac{1}{\beta} [(\Delta \times \mathbf{h}_i^{(1)})^2 + (\Delta \times \mathbf{h}_i^{(2)})^2] + \frac{1}{\kappa} (\mathbf{h}_i^{(1)} + \mathbf{h}_i^{(2)} + \mathbf{f}_i + \Delta s_i)^2 \right\}. \quad (3)$$

Here, $\mathbf{h}^{(a)}$ are integer-valued dual gauge fields, and $\epsilon_{\mu\lambda\nu} \Delta^\nu f_i^\lambda = \delta_{\mu\tau} \eta_i$. Note that we would obtain Eq. (3) both for Eqs. (1) and (2), with $f_i = 0$ for Eq. (2). For Eq. (1) with compact $A_{i\mu}$, s_i is integer-valued. For Eq. (2) with a non-compact $A_{i\mu}$, s_i is real-valued. Therefore in the former case s_i can be gauged away since the $\mathbf{h}^{(a)}$ -fields are integer-valued. We have chosen a gauge where $s_i = 0$. The MC computations were performed using Eqs. (2) and (3). For both Eqs. (2) and (3), we have used $\kappa = \beta$. We have used the standard Metropolis algorithm with periodic boundary conditions on a cubic lattice of size $L \times L \times L$. For Eq. (3) we have used $L = 4, 8, 12, 16, 20, 24, 32, 36, 48, 60, 64, 72, 80, 96, 120$, while for Eq. (2) we have used $L = 48, 64, 80, 96, 112, 120$. A large number of sweeps is required in order to get adequate statistics in the histograms (see below) for the largest system sizes. Firstly, we have computed the second moment of the action $M_2 \equiv \langle (S - \langle S \rangle)^2 \rangle$ for the model with and without a Berry phase term. Secondly, we have focused on a number of quantities that provide information on the character of the phase transition associated with the specific heat anomaly. The first of these quantities is the third moment of the action,

$M_3 \equiv \langle (S - \langle S \rangle)^3 \rangle$. At a second-order phase transition this quantity should scale as follows. The peak-to-peak height scales as $L^{(1+\alpha)/\nu}$, whereas the width between the peaks scales as $L^{-1/\nu}$ [14]. At a first-order phase transition, these quantities scale as L^6 and $L^{-1/\nu}$, respectively [15]. We also study the probability distribution $P(S, L)$ of the action S for various system sizes. At a first-order phase transition, $P(S, L)$ will exhibit a double-peak structure associated with the two coexisting phases.

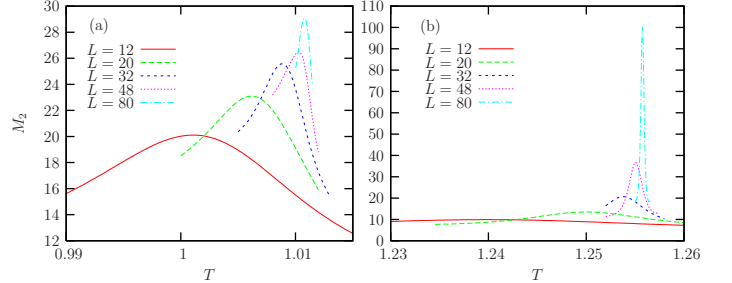


FIG. 1: (Color online) Specific heat M_2 of Eq. (3) for various system sizes. Panel (a): Without Berry phase term. The peak develops into a singularity of the 3DXY type. Panel (b): With Berry phase term. The peak develops into a δ -function singularity with a peak scaling as L^3 , consistent with a first-order phase transition. Note the symmetry and asymmetry of the peaks in the right and left panels, respectively. This is to be expected, since the peaks in the right panel originate with the superposition of a 3DXY peak and an inverted 3DXY peak.

The specific heat M_2 is shown in Fig. 1. Panel (a) shows the anomaly for the model Eq. (3) with no Berry-phase term, i.e., $\Delta \times \mathbf{f} = (0, 0, \eta) = 0$. The anomaly has the characteristic asymmetric shape of the 3DXY model. In this case, there are no Berry phases to suppress the instantons of the compact gauge-field \mathbf{A} at the critical point. Hence, the charged sector does not feature critical fluctuations that can interfere with those of the neutral sector. When the Berry phase field \mathbf{f} is included, the specific heat is notably more symmetric and the anomaly develops into a δ -function peak, consistent with a first-order phase transition. This is shown in panel (b).

To investigate more precisely the character of the phase transition when a Berry phase term is present, we have performed finite-size scaling (FSS) of the third moment of the action, M_3 [14]. The results are shown in Fig. 2, panel (a). It is seen that for small and intermediate system sizes, the height increases with L in a manner which might appear consistent with that of a second-order phase transition. However, the quality of the scaling is not satisfactory, since a clear curvature in the scaling plots is seen (red data points). As system sizes increase we see a gradual increase in the apparent value of $(1 + \alpha)/\nu$, until for large system sizes, we clearly have $M_3 \sim L^6$, consistent with a first-order phase transition [15].

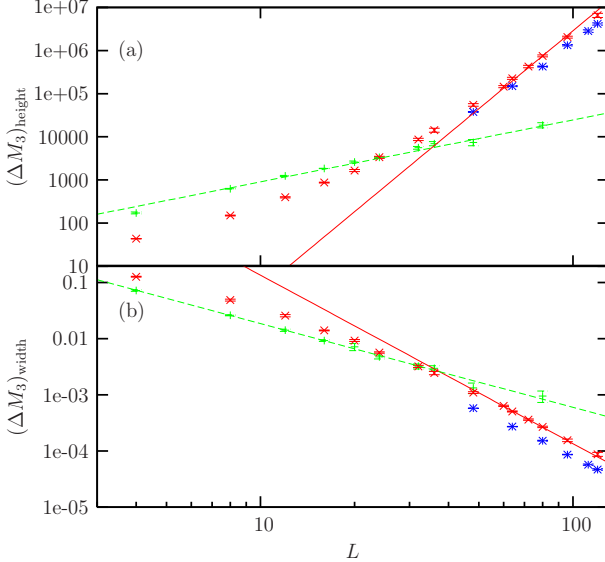


FIG. 2: (Color online) Scaling of the height [panel (a)] and width [panel (b)] of M_3 of the action in Eqs. (2) and (3). The lines in panel (a) represent $L^{1.43}$ and L^6 . The former is the 3DXY result. The lines in panel (b) represent $L^{-1.49}$ and L^{-3} . The former is the 3DXY result. For large system sizes, the height and width scale in manner consistent with a first-order phase transition. Also shown are results for Eq. (3) with no Berry phase term $\mathbf{f} = 0$ (green symbols). These results follow the 3DXY scaling lines. The red symbols are the results for Eq. (3) while the blue symbols are results for Eq. (2).

Panel (b) of Fig. 2 shows the scaling of the width of M_3 . Again, the line with the smallest negative slope is the line one would obtain for the 3DXY model, while the line with the most negative slope is $\sim L^{-3}$, characteristic of a first-order phase transition. Again we obtain apparent scaling, with a crossover regime at intermediate length scales into a regime where the width scales as it would in a first-order phase transition [15]. The results of Fig. 2 provide further support to the notion that the phase transition in the model with a compact gauge field and a Berry phase term is a first-order phase transition.

To investigate this further, we have computed the probability distribution $P(S, L)$ for various system sizes. The results are shown in Fig. 3. Panel (a) shows results for Eq. (1) in the representation Eq. (3). Panel (b) shows results for Eq. (2). The Ferrenberg–Swendsen algorithm has been used to reweight the histograms [16]. For $L \leq 48$, we essentially have not been able to resolve a double peak structure at all, showing that the phase transitions in the models Eqs. (1) and (2) are weakly first-order. We have located the transition temperature from the peak structures in the specific heat and M_3 , and performed long simulations at this temperature for each L . For the largest systems, $L = 96, 120$, up to $120 \cdot 10^6$ sweeps over the lattice were done. A clear double-peak structure in $P(S, L)$ is seen to develop for system sizes

$L > 60$. The fact that such large system sizes are required to bring out the double-peak structure, implies that this phase transition is weakly first-order.

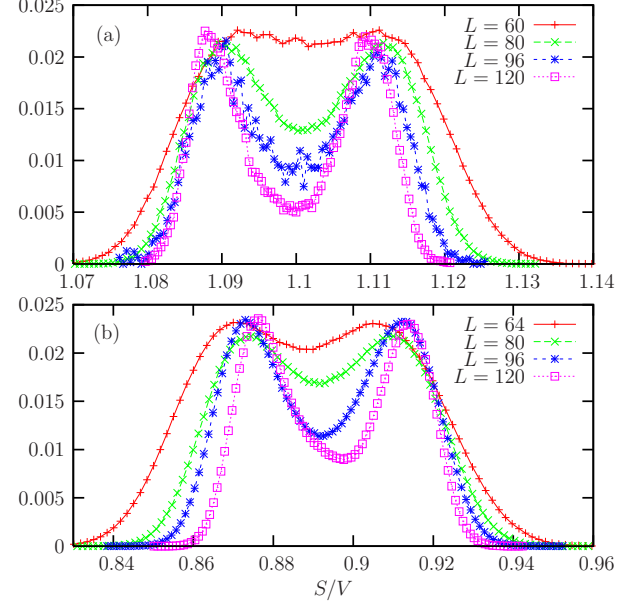


FIG. 3: (Color online) Histograms for the probability distribution $P(S, L)$ as a function of S/L^3 for various system sizes L . (a): results for Eq. (1) in the representation Eq. (3). (b): results Eq. (2). A double peak structure develops with the latent heat per unit volume approaching a finite constant as L is increased. This is a hallmark of a first-order phase transition. For the largest systems, up to $120 \cdot 10^6$ sweeps over the lattice were performed. A total of approximately 500000 CPU hours were used to obtain these results.

We also perform FSS of the height of the peak between the two degenerate minima in the free energy $-\ln[P(S, L)]$. This height should scale as L^2 in a first-order phase transition, since it represents the energy of an area which separates two coexisting phases [17]. The results are shown in panel (a) of Fig. 4. For large enough systems, the height clearly approaches the dotted line $\sim L^2$, as in a first-order transition. This is corroborated by extracting the latent heat per unit volume in the transition, shown in the lower panel of Fig. 4. It approaches a nonzero constant as L is increased, as it should in a first-order phase transition.

Further insight into the nature of the first-order phase transition can be obtained by means of the renormalization group (RG). In the field theory Lagrangian the interaction of the easy-plane system reads $\mathcal{L}_{\text{int}} = u_0(|z_1|^2 + |z_2|^2)^2/2 + v_0|z_1|^2|z_2|^2 = u_0(|z_1|^4 + |z_2|^4)/2 + w_0|z_1|^2|z_2|^2$, where $w_0 = u_0 + v_0$. Consider a generalized situation where the complex fields each have $N/2$ components. A similarly generalized Ginzburg–Landau (GL) theory for superconductors [18] shows that a second-order phase transition occurs only if N is greater than a certain critical value. Thus, we consider the renormalized dimen-

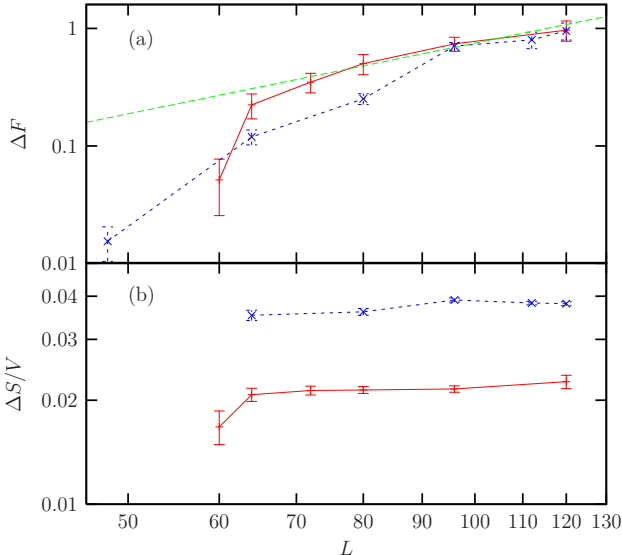


FIG. 4: (Color online) Panel (a) shows the scaling of the height ΔF of the peak between the two minima in $-\ln P(S, L)$ both for Eqs. (3) (red curve) and (2) (blue curve). Dotted line is the line $\sim L^2$. The height scales as $\Delta F \sim L^{d-1}$. This is a hallmark of a first-order phase transition. Panel (b) shows latent heat per unit volume $\Delta S/V$ as a function of L . The upper (blue) curve is from Eq. (2), the lower (red) curve is from Eq. (3). $\Delta S/V$ approaches a nonzero value as L is increased.

sionless couplings in $d = 4 - \varepsilon$ dimensions, $g = u\mu^{-\varepsilon}$, $h = w\mu^{-\varepsilon}$, and f , where f is the dimensionless gauge coupling and μ is an arbitrary mass scale. The β functions at one-loop order are [19] $\beta_g = -\varepsilon g - 6gf + (N + 8)g^2/2 + 2Nh^2 + 6f^2$, $\beta_h = -\varepsilon h - 6hf + 3(N + 2)gh + 6f^2$, and $\beta_f = -\varepsilon f + Nf^2/3$. For all values of N no fixed points such that $h = 0$ and $f = 3\varepsilon/N$ exist. For $N \geq 2$ and $f = 0$ there are two fixed points with $h \neq 0$, the infrared stable one corresponding to $h > 0$. Two fixed points with $f = 3\varepsilon/N$ and $h < 0$ are found for $N \geq 300$, one of which is infrared stable while the other one is unstable and associated with multicritical behavior. In the GL theory, the existence of a critical value of N above which an infrared stable fixed point is found reflects the strong-coupling behavior for $N = 2$, though being unable to reproduce it: actually it turns out that the phase transition for $N = 2$ is second-order in the type II regime [12], while a first-order phase transition occurs in the type I regime, thus establishing the existence of a tricritical point in the phase diagram [20, 21]. The same may occur here, which would apparently contradict the results of the MC simulations; see also Ref. [13] for another simulation in a closely related model which also leads to a first-order phase transition. However, it should be emphasized that the present simulation is made in the *deep* easy-plane limit, i.e., the limit where $|z_1|^2 - |z_2|^2 \approx 0$ at the core of the meron vortices. This limit is not assumed in the RG analysis. In order to see if the large

N result really reflects the actual strong-coupling behavior of the $N = 2$ theory, a nonperturbative approach is needed. MC simulations of the type done in Ref. [21] is a promising alternative.

This work was supported by the Research Council of Norway, Grant Nos. 158518/431, 158547/431, 167498/V30 (STORFORSK), and 167498/V30 (NANOMAT), and the Norwegian High-Performance Computing Consortium (NOTUR).

[1] K. G. Wilson and J. B. Kogut, Phys. Rep. **12** C, 75 (1974).
[2] T. Senthil, A. Vishwanath, L. Balents, S. Sachdev, and M. P. A. Fisher, Science, **303**, 1490 (2004).
[3] T. Senthil, L. Balents, S. Sachdev, A. Vishwanath, and M. P. A. Fisher, Phys. Rev. **B 70**, 144407 (2004).
[4] S. Sachdev, in: “Quantum magnetism”, U. Schollwock, J. Richter, D. J. J. Farnell and R. A. Bishop, eds., Lecture Notes in Physics (Springer, Berlin 2004).
[5] N. Read and S. Sachdev, Phys. Rev. Lett., **62**, 1694 (1989); Phys. Rev. B **42**, 4568 (1990).
[6] S. Sachdev and R. Jalabert, Mod. Phys. Lett., **B 4**, 1043 (1990).
[7] A. M. Polyakov, Nucl. Phys. B **120**, 429 (1977).
[8] E. Fradkin and S. H. Shenker, Phys. Rev. D **19**, 3682 (1979).
[9] E. Babaev, Phys. Rev. Lett. **89** (2002) 067001; Nucl. Phys. B **686** (2004) 397.
[10] J. Smiseth, E. Smørgrav, and A. Sudbø, Phys. Rev. Lett. **93**, 077002 (2004); E. Smørgrav, E. Babaev, J. Smiseth, and A. Sudbø, Phys. Rev. Lett. **95**, 135301 (2005); E. Smørgrav, J. Smiseth, E. Babaev, and A. Sudbø, Phys. Rev. Lett. **94**, 096401 (2005); J. Smiseth, E. Smørgrav, E. Babaev, and A. Sudbø, Phys. Rev. **B 71**, 214509 (2005).
[11] M. B. Einhorn and R. Savit, Phys. Rev. **D 19**, 1198 (1979).
[12] C. Dasgupta and B. I. Halperin, Phys. Rev. Lett. **47**, 1556 (1981).
[13] A. B. Kuklov, N. V. Prokof’ev, B. V. Svistunov, and M. Troyer, Ann. Phys. (N.Y.) **321**, 1602 (2006); O. I. Motrunich and A. Vishwanath, Phys. Rev. B **70**, 075104 (2004).
[14] A. Sudbø, E. Smørgrav, J. Smiseth, F. S. Nogueira, and J. Hove, Phys. Rev. Lett. **89**, 226403 (2002); J. Smiseth, E. Smørgrav, F. S. Nogueira, J. Hove, and A. Sudbø, Phys. Rev. B **67**, 205104 (2003).
[15] M. E. Fisher and A. N. Berker, Phys. Rev. B **26**, 2507 (1982); J. L. Cardy and P. Nightingale, Phys. Rev. B **27**, 4256 (1983).
[16] A. M. Ferrenberg and R. H. Swendsen, Phys. Rev. Lett., **61**, 2635 (1988); *ibid* **63**, 1195 (1989).
[17] J. Lee and J. M. Kosterlitz, Phys. Rev. Lett. **65**, 137 (1990).
[18] B. I. Halperin, T. C. Lubensky, and S.-K. Ma, Phys. Rev. Lett., **32**, 292 (1974).
[19] F. S. Nogueira, S. Kragset, and A. Sudbø, in preparation.
[20] H. Kleinert, Lett. Nuovo Cimento **35**, 405 (1982).
[21] S. Mo, J. Hove, and A. Sudbø, Phys. Rev. B **65**, 104501 (2002).